

Modeling of Nonequilibrium Processes behind a Shock Wave in a Mixture of Carbon Dioxide and Argon

S. A. Batalov^{a,*} and E. V. Kustova^{a,**}

^a St. Petersburg University, St. Petersburg, 199034 Russia

* e-mail: st076569@student.spbu.ru

** e-mail: e.kustova@spbu.ru

Received October 15, 2022; revised November 16, 2022; accepted November 17, 2022

Abstract—A closed self-consistent model of a nonequilibrium flow of a mixture of carbon dioxide and argon behind the front of a plane shock wave is developed. The generalized Chapman–Enskog method in the three-temperature approach, which takes into account different channels of vibrational relaxation in a carbon-dioxide molecule, is used. An extended system of Navier–Stokes–Fourier equations consisting of mass-, momentum-, and energy-conservation equations supplemented by diffusion equations for the mixture components and relaxation equations for vibrational modes of the CO₂ molecule are written. Constitutive relations for the stress tensor, diffusion velocity, heat flux, and vibrational energy fluxes are obtained. An algorithm for calculating the coefficients of shear and bulk viscosity, the thermal conductivity of different degrees of freedom, diffusion and thermal diffusion are developed and implemented. The model is validated by comparing calculated transport coefficients with experimental data for the viscosity and thermal conductivity of carbon dioxide and argon and for the binary diffusion coefficient. Good agreement with the experiment is obtained. The dependence of transport coefficients on the gas temperature, vibrational-mode temperatures, and mixture composition is analyzed. The developed model is ready for use in the numerical simulation of shock waves in a CO₂–Ar mixture.

Keywords: transport coefficients, three-temperature model, shock wave, carbon dioxide, argon

DOI: 10.1134/S1063454123020024

1. INTRODUCTION

The numerical modeling of highly nonequilibrium processes in mixtures of reacting gases is important for simulating the reentry of descent vehicles into the atmosphere of planets, high-speed flights, and environmental problems. In recent years, much attention has been paid to the study of nonequilibrium flows of carbon dioxide, the main component of the atmosphere of Mars, as well as an undesirable product of human-made activity [1].

Depending on the degree of deviation from equilibrium, detailed state-to-state and reduced multitemperature models can be used to describe the flow [2]. The multitemperature model of nonequilibrium flows is of great practical interest because it is more computationally efficient. Recent works [3–5] presented the results and methods for modeling the nonequilibrium flow of a viscous single-component carbon dioxide. For example, in [3], a multitemperature model of the relaxation processes in CO₂ behind the shock wave was developed and implemented in a 1D formulation taking into account shear and bulk viscosity, thermal conductivity of translational, rotational, and vibrational degrees of freedom as well as various channels of vibrational energy relaxation of carbon-dioxide molecules, including intramode and intermode exchanges. A limitation of this model is that it is constructed for a pure gas and does not describe diffusion processes.

Modeling of gas flows behind a shock wave is one of benchmark problems that makes it possible to assess various theoretical approaches and determine their limits of applicability: classical and extended Navier–Stokes–Fourier equations, momentum methods, and direct statistical modeling [3, 6–9]. For model validation, experimental data are commonly used. Whereas a sufficient number of reliable experimental results are available for monoatomic gases and air components [10–12], there are almost no experimental data for CO₂. An exception is [13], in which the flow of a CO₂–Ar mixture behind a shock wave was investigated.

In the present work, we generalize the theoretical model proposed in [3] by adding one more component, argon, in order to subsequently compare with the experimental results of [13] and validate models of kinetics and transport processes in carbon dioxide. In order to solve this problem, we use a multitemperature model for a mixture of gases taking into account the internal vibrational degrees of freedom of CO₂ molecules and without taking into account electronic excitation. In the model, the equations of conservation of mass, momentum, and energy are supplemented by relaxation equations for the vibrational energy of the combined (symmetric–deformation) and asymmetric modes of a CO₂ molecule as well as diffusion equations for the mixture components. An important part of the model is the algorithms for calculating the transport coefficients, i.e., viscosity, thermal conductivity, and diffusion, constructed by rigorous methods of the kinetic theory of gases [2].

2. THREE-TEMPERATURE MODEL

In order to describe transport and relaxation processes in nonequilibrium rarefied gases, there are two principal approaches: state-to-state and multitemperature [2]. We will focus on the second approach, because it is simpler to implement (in this approach, nonequilibrium kinetics is described using a smaller number of equations) and, therefore, is of greater practical interest. A necessary step in modeling is the construction of a closed system of equations for fluid-dynamic parameters.

2.1. Equations for Fluid-Dynamic Parameters

Let us write down a system of equations for the dynamics of a multicomponent mixture in the 1D formulation (we consider the quasi one dimensional problem of shock-wave propagation) in the absence of chemical reactions. It consists of the continuity equation, equations for the concentrations of chemical components, equations of the conservation of momentum and total energy, and additional relaxation equations.

$$\frac{\partial \rho}{\partial t} + \frac{\partial}{\partial x}(\rho v) = 0, \quad (1)$$

$$\frac{\partial \rho_{\text{CO}_2}}{\partial t} + \frac{\partial}{\partial x}(\rho_{\text{CO}_2}(v + V_{\text{CO}_2})) = 0, \quad (2)$$

$$\rho \left(\frac{\partial v}{\partial t} + v \frac{\partial v}{\partial x} \right) + \frac{\partial P_{xx}}{\partial x} = 0, \quad (3)$$

$$\rho \left(\frac{\partial E}{\partial t} + v \frac{\partial E}{\partial x} \right) + \frac{\partial q}{\partial x} + P_{xx} \frac{\partial v}{\partial x} = 0, \quad (4)$$

$$\rho_{\text{CO}_2} \left(\frac{\partial E_{12}}{\partial t} + v \frac{\partial E_{12}}{\partial x} \right) + \frac{\partial q_{12}}{\partial x} = R_{12} + E_{12} \frac{\partial}{\partial x}(\rho_{\text{CO}_2} V_{\text{CO}_2}), \quad (5)$$

$$\rho_{\text{CO}_2} \left(\frac{\partial E_3}{\partial t} + v \frac{\partial E_3}{\partial x} \right) + \frac{\partial q_3}{\partial x} = R_3 + E_3 \frac{\partial}{\partial x}(\rho_{\text{CO}_2} V_{\text{CO}_2}). \quad (6)$$

Here, ρ_c and n_c are the mass and number densities of particles of the gas of the corresponding chemical species c ; ρ is the mixture density; v is the flow velocity; p is the gas pressure; E , E_{12} , and E_3 are the total energy and energy of vibrational modes in a unit mass of gas; V_c are the species diffusion velocities; P_{xx} is the stress-tensor component included in the equations in the 1D formulation; q , q_{12} , and q_3 are the components of the vectors of the heat flux and vibrational energy fluxes in various modes; R_{12} and R_3 are the vibrational relaxation rates; k is the Boltzmann constant; and T is the temperature of the translational motion of particles. The densities and concentrations are related by the following relations:

$$\rho = \rho_{\text{CO}_2} + \rho_{\text{Ar}}, \quad n = n_{\text{CO}_2} + n_{\text{Ar}}, \quad \rho_c = m_c n_c. \quad (7)$$

Here, m_c is the mass of a particle of the chemical species c . The energies, as well as the flow and relaxation terms, are described in the following sections.

It is important to note that when considering (1) symmetric, (2) bending, and (3) asymmetric vibrational modes of the CO₂ molecule, we introduce the unique temperature T_{12} and energy E_{12} for modes 1 and 2 due to the fact that in real flows they are rapidly equilibrated. The asymmetric mode is described by

the intrinsic temperature T_3 and vibrational energy E_3 . The equilibrium is achieved by intramode and intermode exchanges of the vibrational energy [5].

In contrast to [3], in this study, diffusion processes are taken into account; therefore, the diffusion velocity V_c of the corresponding species appears in the equations for the macroparameters. In addition, the specific energies and transport coefficients not only depend on T , T_{12} , and T_3 , but are also functions of the molar fractions of the mixture components.

2.2. Equations of State

In order to close the system of gas-dynamic equations, it is necessary to write the thermal and caloric equations of state. We consider the model of a thermally perfect gas, $p = nkT$, and a calorically imperfect gas. Expressions for the specific internal energy are derived in the frame of the multitemperature approach:

$$\rho E = \frac{3}{2}kT(n_{\text{CO}_2} + n_{\text{Ar}}) + \rho_{\text{CO}_2}(E_{\text{rot}} + E_{12} + E_3), \quad (8)$$

$$E_{\text{rot}} = \frac{kT}{m_{\text{CO}_2}}, \quad (9)$$

$$E_{12} = \frac{1}{m_{\text{CO}_2}Z_{12}(T_{12})} \sum_{i_1, i_2} s_{i_1, i_2} \varepsilon_{i_1, i_2} \exp\left(-\frac{\varepsilon_{i_1, i_2}}{kT_{12}}\right), \quad (10)$$

$$E_3 = \frac{1}{m_{\text{CO}_2}Z_3(T_3)} \sum_{i_3} s_{i_3} \varepsilon_{i_3} \exp\left(-\frac{\varepsilon_{i_3}}{kT_3}\right). \quad (11)$$

Here, E_{rot} is the specific rotational energy, $s_{i_1, i_2} = i_2 + 1$ and $s_{i_3} = 1$ are the statistical weights of the combined and asymmetric modes, and $Z_{12}(T_{12})$ and $Z_3(T_3)$ are the corresponding vibrational partition functions. Based on the results of the study [3], we can write the following:

$$Z_{12} = \sum_{i_1, i_2} s_{i_1, i_2} \exp\left(-\frac{\varepsilon_{i_1, i_2}}{kT_{12}}\right), \quad Z_3 = \sum_{i_3} s_{i_3} \exp\left(-\frac{\varepsilon_{i_3}}{kT_3}\right), \quad (12)$$

where the vibrational energies in the combined and asymmetric modes are as follows

$$\varepsilon_{i_1, i_2} = (2i_1 + i_2)\varepsilon_{010}, \quad \varepsilon_{i_3} = i_3\varepsilon_{001}, \quad (13)$$

i_1 , i_2 , and i_3 are the quantum numbers of vibrational modes of the CO_2 molecule, and ε_{010} and ε_{001} are the vibrational energies of corresponding states.

2.3. Transport and Relaxation Terms

In order to completely close the system, it is necessary to write the transport and relaxation terms in Eqs. (1)–(6). In the first-order approximation of the generalized Chapman–Enskog method [2], the heat flux q is given by the following expression

$$q = q_{\text{tr,rot}} + q_{12} + q_3 + q_{\text{diff}}. \quad (14)$$

Here, the translational and rotational energy fluxes, the energies of the combined and asymmetric vibrational modes, and the heat flux due to diffusion were obtained as follows:

$$q_{\text{tr,rot}} = -\lambda'(T, n_{\text{CO}_2}, n_{\text{Ar}}) \frac{\partial T}{\partial x}, \quad (15)$$

$$q_{12} = -\lambda_{12}(T_{12}, T) \frac{\partial T_{12}}{\partial x}, \quad (16)$$

$$q_3 = -\lambda_3(T_3, T) \frac{\partial T_3}{\partial x}, \quad (17)$$

$$q_{\text{diff}} = \sum_c (\rho_c h_c V_c - p D_{T_c} d_c), \quad (18)$$

where λ_{12} , λ_3 , and λ' are the thermal conductivity coefficients (for vibrational and translational–rotational modes), and D_{T_c} are the thermal diffusion coefficients for each chemical species. The specific enthalpy of the components is given by the following expressions

$$h_{\text{CO}_2} = \frac{5}{2} \frac{kT}{m_{\text{CO}_2}} + E_{\text{rot}} + E_{12} + E_3, \quad h_{\text{Ar}} = \frac{5}{2} \frac{kT}{m_{\text{Ar}}}. \quad (19)$$

Expressions for the diffusion velocity and diffusive driving force are

$$V_c = -\sum_d D_{cd} d_d - D_{T_c} \frac{\partial}{\partial x} \ln T, \quad (20)$$

$$d_c = \frac{\partial}{\partial x} \left(\frac{n_c}{n} \right) + \left(\frac{n_c}{n} - \frac{\rho_c}{\rho} \right) \frac{\partial}{\partial x} \ln p, \quad (21)$$

here D_{cd} are diffusion coefficients.

The component of the stress tensor [3] can be written as follows:

$$P_{xx} = p - \left(\frac{4}{3} \eta(T, n_{\text{CO}_2}, n_{\text{Ar}}) + \zeta(T, n_{\text{CO}_2}, n_{\text{Ar}}) \right) \frac{\partial v}{\partial x}. \quad (22)$$

Here, η and ζ are shear and bulk viscosity coefficients, respectively. Note that the introduction of bulk viscosity into the Navier–Stokes–Fourier equations noticeably affects the macroparameter profiles in the shock-wave front [3, 6]; the density profiles for diatomic gases appear to be noticeably closer to those measured experimentally. It also should be noted that bulk viscosity has not previously been considered in the equations for a mixture flow behind the shock-wave front; in this study it is the first time this has been done.

Relaxation in the combined and asymmetric modes [2] includes the contribution of the intramode exchange of the translational and vibrational energy $V T_2$ as well as the intermode energy exchanges $V V_{2-3}$ and $V V_{1-2-3}$ between the asymmetric and other vibrational modes:

$$R_{12} = R_{12}^{V T_2} + R_{12}^{V V_{2-3}} + R_{12}^{V V_{1-2-3}}, \quad (23)$$

$$R_3 = R_3^{V V_{2-3}} + R_3^{V V_{1-2-3}}. \quad (24)$$

The vibrational relaxation rate in each mode R_{12} and R_3 can be calculated using the modified Landau–Teller equation or the advanced multitemperature models proposed in [14].

2.4. Transport Coefficients

The application of the generalized Chapman–Enskog method makes it possible to express transport coefficients in terms of expansion coefficients of the first-order distribution function in series of orthogonal Sonine and Waldmann–Trübenbacher polynomials [2]. For the coefficients of shear and bulk viscosity, multicomponent diffusion, and thermal diffusion, we obtain

$$\eta = \frac{kT}{2} \sum_c x_c b_{c,0}, \quad \zeta = -kT (x_{\text{CO}_2} f_{\text{CO}_2,10} + x_{\text{Ar}} f_{\text{Ar},1}), \quad (25)$$

$$D_{cd} = \frac{1}{2n} d_{c,0}^d, \quad D_{T_{\text{CO}_2}} = -\frac{1}{2n} a_{\text{CO}_2,00}, \quad D_{T_{\text{Ar}}} = -\frac{1}{2n} a_{\text{Ar},0}. \quad (26)$$

Here, $x_c = n_c/n$, the expansion coefficients $b_{c,0}$, $d_{c,0}^d$, $a_{c,rp}$, and $f_{c,rp}$ are determined from the solution of the corresponding systems of linear equations [5]. We write out here only the simplest system for the shear viscosity coefficient η . Transport:

$$\begin{pmatrix} H_{00}^{\text{CO}_2-\text{CO}_2} & H_{00}^{\text{CO}_2-\text{Ar}} \\ H_{00}^{\text{Ar}-\text{CO}_2} & H_{00}^{\text{Ar}-\text{Ar}} \end{pmatrix} \times \begin{pmatrix} b_{\text{CO}_2,0} \\ b_{\text{Ar},0} \end{pmatrix} = \begin{pmatrix} \frac{2}{kT} x_{\text{CO}_2} \\ \frac{2}{kT} x_{\text{Ar}} \end{pmatrix}. \quad (27)$$

Table 1. Equilibrium coefficients of shear viscosity ($\eta \times 10^6$ Pa s) and thermal conductivity ($\lambda \times 10^3$ W/m K) for pure CO₂ and Ar

T, K	CO ₂					Ar				
	η			λ		η			λ	
	[15]	[17]	calc	[15]	calc	[15]	[17]	calc	[15]	calc
300	15.3	15.0	15.2	16.6	18.2	22.7	22.7	22.4	17.7	17.5
400	19.8	19.5	19.7	24.3	26.1	28.9	28.5	28.3	22.2	22.1
500	23.7	23.6	23.8	32.5	33.8	34.2	33.6	33.5	26.6	26.1
600	27.3	33.9	27.7	40.7	41.5	38.9	38.3	38.3	30.7	29.9
700	30.7	—	31.2	48.1	48.9	43.3	—	42.8	34.1	33.4
800	33.8	39.5	34.6	55.4	56.1	47.4	46.4	47.1	37.4	36.7
900	36.8	—	37.8	62.0	63.0	51.4	—	51.1	40.6	39.9
1000	39.5	—	40.8	68.3	69.7	55.1	53.5	54.9	43.6	42.9

The systems for the remaining coefficients have a similar form [5]. Let us now define the coefficients of the system matrix (integral brackets):

$$H_{00}^{cd} = \frac{16 x_c x_d}{5 k T} \frac{m_c m_d}{(m_c + m_d)^2} \left(-\frac{10}{3} \Omega_{cd}^{(1,1)} + \Omega_{cd}^{(2,2)} \right), \quad d \neq c, \quad (28)$$

$$H_{00}^{cc} = \frac{16}{5} \sum_{c \neq b} \frac{x_c x_b}{k T} \frac{m_b}{(m_c + m_b)^2} \left(\frac{10}{3} \Omega_{cb}^{(1,1)} m_c + \Omega_{cb}^{(2,2)} m_b \right) + \frac{8 x_c^2}{5 k T} \Omega_c^{(2,2)}. \quad (29)$$

Here, $\Omega_{cd}^{(1,1)}$ and $\Omega_{cd}^{(2,2)}$ are standard Ω -integrals [2]. Integral brackets for other systems are defined in the same way.

Next, let us write down expressions for the thermal conductivity coefficients:

$$\lambda' = \lambda_{tr} + \lambda_{rot}, \quad \lambda_{tr} = \frac{5}{4} k (x_{CO_2} a_{CO_2,10} + x_{Ar} a_{Ar,1}), \quad \lambda_{rot} = \frac{m_{CO_2} n_{CO_2} c_{rot}}{\sum_c \frac{x_c}{\mathcal{D}_{CO_2c}}}, \quad (30)$$

$$\lambda_{12} = \frac{m_{CO_2} n_{CO_2} c_{12}}{\sum_c \frac{x_c}{\mathcal{D}_{CO_2c}}}, \quad \lambda_3 = \frac{m_{CO_2} n_{CO_2} c_3}{\sum_c \frac{x_c}{\mathcal{D}_{CO_2c}}}. \quad (31)$$

Here, $c_{rot} = k/m_{CO_2}$ is the specific heat of the rotational degrees of freedom, and $c_{12} = \partial E_{12}/\partial T_{12}$ and $c_3 = \partial E_3/\partial T_3$ are the specific heats of vibrational degrees of freedom. The expression for the binary diffusion coefficient is as follows

$$\mathcal{D}_{cd} = \frac{3kT}{16nm_{cd}} \frac{1}{\Omega_{cd}^{(1,1)}}, \quad (32)$$

$m_{cd} = m_c m_d / (m_c + m_d)$ is the reduced mass of particles of species c and d .

Therefore, at this stage, a closed theoretical multitemperature model describing the 1D nonequilibrium flow of the CO₂–Ar mixture is constructed. For the first time, the model simultaneously takes into account different channels of vibrational relaxation, diffusion and thermal diffusion processes, and the bulk viscosity of the mixture. The numerical solution of Eqs. (1)–(6) will be carried out in further studies.

3. CALCULATION OF THE TRANSPORT COEFFICIENTS

An algorithm for calculating all the transport coefficients of the mixture (shear and bulk viscosity, diffusion, thermal diffusion, and thermal conductivity) was implemented in this work. When calculating the transport coefficients, the Lennard–Jones interaction potential was used to find the Ω -integrals.

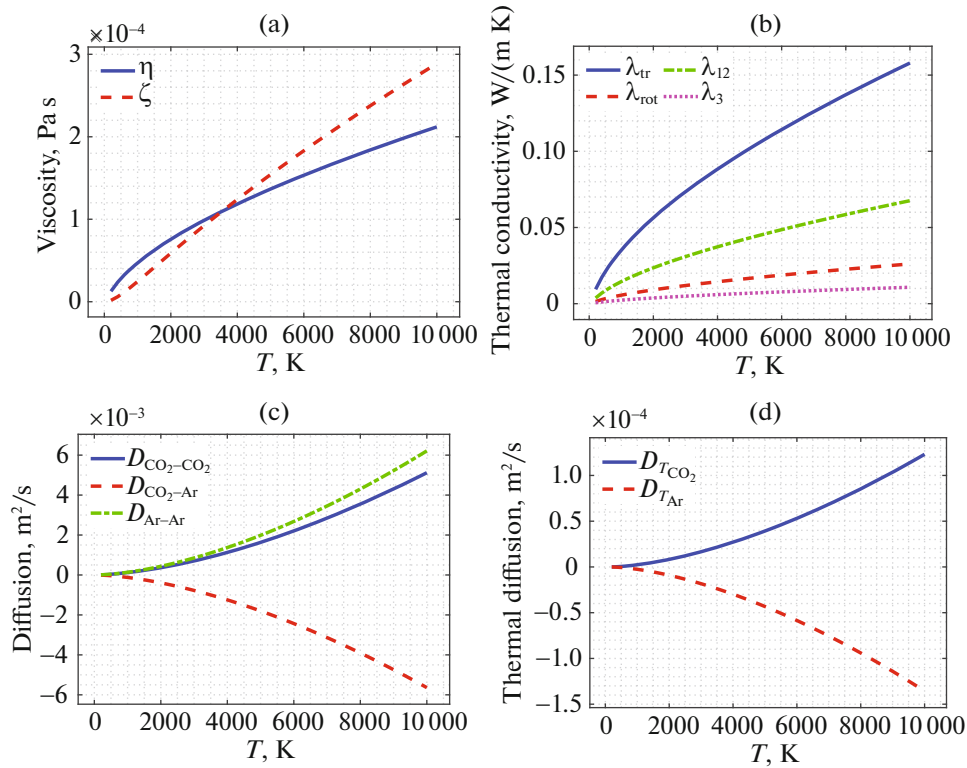


Fig. 1. Transport coefficients as functions of temperature: (a) $\eta(T)$, $\zeta(T)$; (b) $\lambda_{tr}(T)$, $\lambda_{rot}(T)$, $\lambda_{12}(T)$, $\lambda_3(T)$; (c) $D_{cd}(T)$; (d) $D_{T_c}(T)$.

In order to validate the model, the thermal conductivity and shear viscosity coefficients for pure carbon dioxide and argon, and the binary diffusion coefficient for the mixture were calculated. In Table 1, the coefficients of thermal conductivity and shear viscosity measured experimentally [15, 16] and obtained numerically are presented in the case of equilibrium ($T = T_{12} = T_3$) at a pressure of $p = 1 \text{ bar} = 10^5 \text{ Pa}$. Also in Table 1, data for the viscosity coefficients from [17] are given. In this case, the total thermal conductivity coefficient of CO_2 is obtained by summing the coefficients $\lambda(T) = \lambda'(T) + \lambda_{12}(T) + \lambda_3(T)$. The comparison shows that for argon, the deviation of the shear viscosity coefficient from the experimental data is (1, 2%), where the first value is the mean deviation and the second is the maximum deviation. For the thermal conductivity coefficient, the mean and maximum deviations are (2, 3%). Therefore, the calculated coefficients for argon agree well with experiment. For carbon dioxide, in the considered range of conditions, the deviations for the shear viscosity coefficient are (2, 3%) and for the thermal conductivity coefficient, (4, 10%); the deviation decreases with increasing temperature.

Table 2 shows the values of the binary diffusion coefficient for different gas temperatures obtained numerically and based on empirical formula [17]; the mixture pressure is equal to the atmospheric one, which is $p = 101\,300 \text{ Pa}$. It should be noted that with increasing temperature the deviation of the calculated value of the binary diffusion coefficient from the experimental one slightly increases and reaches $\approx 10\%$ at $T = 1000 \text{ K}$. In this article, the Lennard–Jones potential is used; for temperatures above 1000 K, the Born–Mayer potential is planned to be used in the future to improve the accuracy. Nevertheless, the dif-

Table 2. Binary diffusion coefficient ($\mathcal{D}_{\text{CO}_2\text{-Ar}}$ cm²/s) for the $\text{CO}_2\text{-Ar}$ mixture

T , K	300	400	500	600	700	800	900	1000
Calc	0.14	0.24	0.37	0.51	0.66	0.84	1.02	1.23
[17], 3–10%	0.15	0.27	0.4	0.56	0.73	0.93	1.14	1.37
Δ , %	6.2	7.8	8.7	9.3	9.8	10.1	10.4	10.6

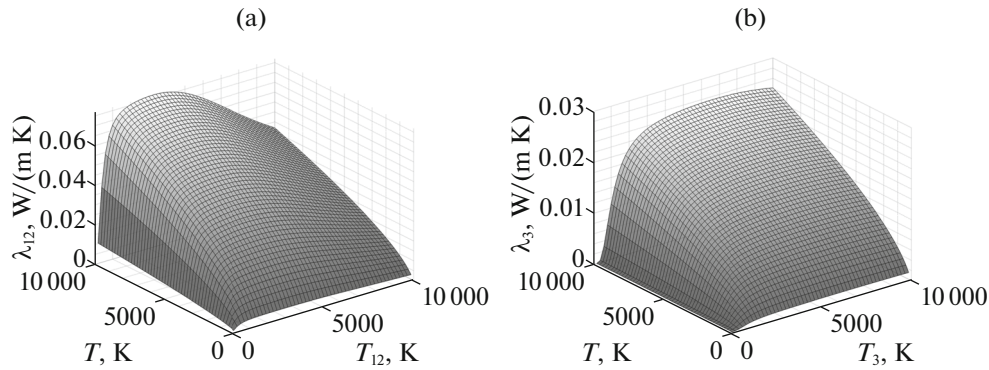


Fig. 2. Thermal conductivity coefficients: (a) $\lambda_{12}(T, T_{12})$ and (b) $\lambda_3(T, T_3)$.

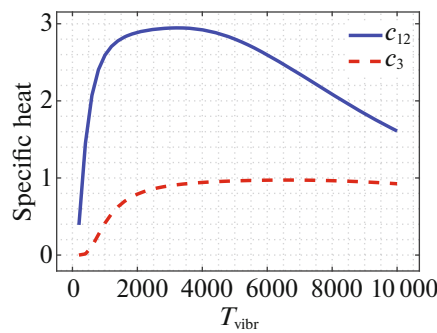


Fig. 3. Dimensionless vibrational specific heats $c_{12}(T_{12})$, $c_3(T_3)$.

ference from the results of [17] does not exceed the approximation error; therefore, the obtained results can be considered satisfactory and recommended for use in further calculations.

Figures 1 and 2 show the viscosity, thermal conductivity, diffusion, and thermal diffusion coefficients for $x_{\text{CO}_2} = x_{\text{Ar}} = 0.5$ and $p = 101\,300$ Pa. The vibrational thermal conductivity coefficients are calculated for $T_{12} = T_3 = 1000$ K.

It is important to note that the bulk viscosity coefficient ζ does not differ significantly in magnitude from the shear viscosity coefficient η over the entire temperature range, i.e., its contribution is significant. The rotational thermal conductivity coefficient λ_{rot} makes a small contribution to energy transfer, unlike the translational thermal conductivity coefficient λ_{tr} , and is close to the asymmetric mode thermal conductivity coefficient λ_3 both in trend and magnitude. It should be noted that a significant contribution to thermal conductivity is made by the coefficient λ_{12} , and it behaves nonmonotonically with increasing vibrational temperature T_{12} , in contrast to the coefficient λ_3 . This nonmonotonicity is caused by the behavior of the vibrational specific heat $c_{T_{12}}$ at high temperatures, which is confirmed by Fig. 3, which shows the dependence of vibrational specific heats on the corresponding vibrational temperatures.

Figure 4 shows the transport coefficients for different fractions of argon in the mixture; it is assumed that $T = T_{12} = T_3 = 5000$ K and $p = 101\,300$ Pa. Note that the bulk viscosity coefficient ζ decreases with an increase in the molar fraction of argon; this is natural because the energy stored in the internal degrees of freedom decreases; the contribution of the translational thermal conductivity increases, and the contribution of the others decreases. Self-diffusion coefficients depend significantly on the component concentrations decreasing as the molar fraction of the corresponding component increases. The thermal diffusion coefficients increase with increasing molar fraction of argon.

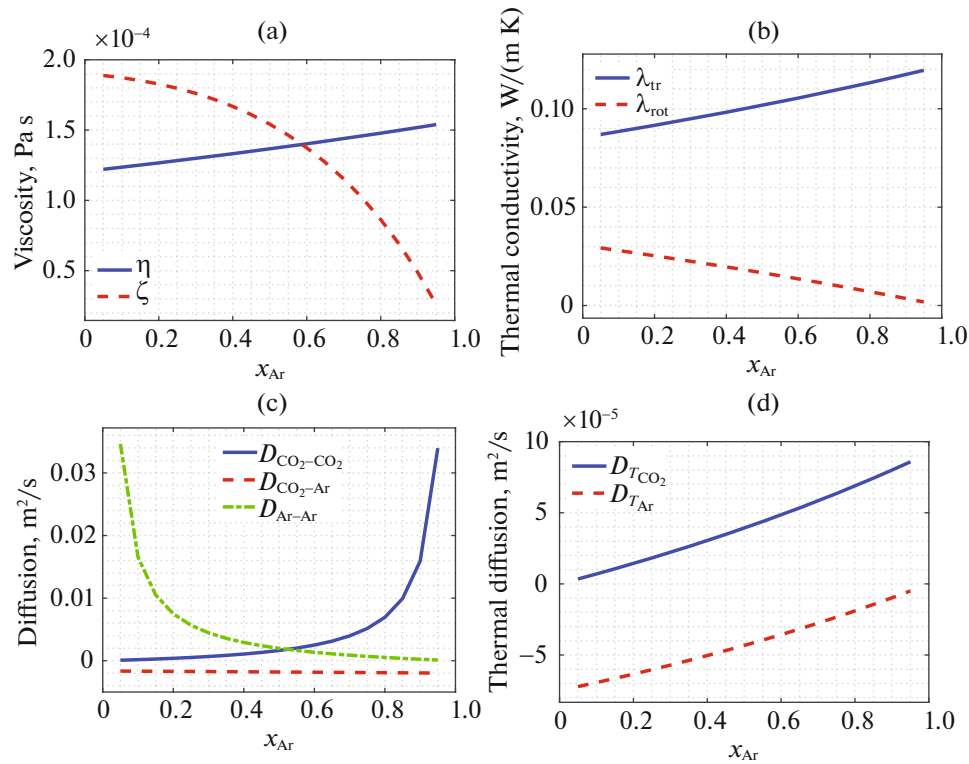


Fig. 4. Dependence of the transport coefficients on the molar fraction of argon: (a) $\eta(x_{Ar})$, $\zeta(x_{Ar})$; (b) $\lambda_{tr}(x_{Ar})$, $\lambda_{rot}(x_{Ar})$; (c) $D_{cd}(x_{Ar})$; (d) $D_{T_c}(x_{Ar})$.

4. CONCLUSIONS

In this work, we developed a theoretical three-temperature model of the nonequilibrium flow of a CO_2 –Ar mixture and implemented an algorithm for calculating transport coefficients, namely, the coefficients of thermal conductivity, shear and bulk viscosity, diffusion, and thermal diffusion. The model was validated using the shear viscosity and thermal conductivity coefficients for pure argon and carbon dioxide separately and the binary diffusion coefficient as examples. For Ar, the mean error is less than 2% for both coefficients; for carbon dioxide, the model gives good agreement for the shear viscosity coefficient (average deviation of about 3%), but for the thermal conductivity coefficient, on average, there is a somewhat stronger discrepancy, about 4–5%. In general, the agreement with the experiment is satisfactory, and the model can be recommended for use. The developed algorithm will be used in future studies for numerical simulations of the flow of the CO_2 –Ar mixture in a shock wave and for comparison of the results with the experiment.

FUNDING

This work was supported by St. Petersburg State University, project no. 93022273.

CONFLICT OF INTEREST

The authors declare that they have no conflicts of interest.

REFERENCES

1. L. D. Pietanza, O. Guitella, V. Aquilanti, and I. Armenise, “Advances in non-equilibrium CO_2 plasma kinetics: A theoretical and experimental review,” *Eur. Phys. J. D* **75**, 237 (2021). <https://doi.org/10.1140/epjd/s10053-021-00226-0>
2. E. A. Nagnibeda and E. V. Kustova, *Nonequilibrium Reacting Gas Flows: Kinetic Theory of Transport and Relaxation Processes* (Springer, Berlin, 2009).

3. I. Alekseev and E. Kustova, “Extended continuum models for shock waves in CO₂,” *Phys. Fluids* **33**, 096101 (2021).
4. I. V. Alekseev and E. V. Kustova, “Numerical simulations of shock waves in viscous carbon dioxide flows using finite volume method,” *Vestn. St. Petersburg Univ: Math.* **53**, 500–510 (2020).
<https://doi.org/10.1134/S1063454120030024>
5. E. V. Kustova and E. A. Nagnibeda, “On a correct description of a multi-temperature dissociating CO₂ flow,” *Chem. Phys.* **321**, 293–310 (2006).
6. T. Elizarova, A. Khokhlov, and S. Montero, “Numerical simulation of shock wave structure in nitrogen,” *Phys. Fluids* **19**, 068102 (2007).
7. M. Y. Timokhin, H. Struchtrup, A. A. Kokhanchik, and Y. A. Bondar, “Different variants of R13 moment equations applied to the shock-wave structure,” *Phys. Fluids* **29**, 037105 (2017).
8. G. V. Shoen, M. Y. Timokhin, and Y. A. Bondar, “On the total enthalpy behavior inside a shock wave,” *Phys. Fluids* **32**, 041703 (2020).
9. I. Wysong, S. Gimelshein, Y. Bondar, and M. Ivanov, “Comparison of direct simulation Monte Carlo chemistry and vibrational models applied to oxygen shock measurements,” *Phys. Fluids* **26**, 043101 (2014).
10. H. Alsmeyer, “Density profiles in argon and nitrogen shock waves measured by the absorption of an electron beam,” *J. Fluid Mech.* **74**, 497–513 (1976).
11. L. B. Ibraguimova, A. L. Sergievskaya, V. Yu. Levashov, O. P. Shatalov, Yu. V. Tunik, and I. E. Zabelinskii, “Investigation of oxygen dissociation and vibrational relaxation at temperatures 4000–10800 K,” *J. Chem. Phys.* **139**, 034317 (2013).
<https://doi.org/10.1063/1.4813070>
12. J. W. Streicher, A. Krish, and R. K. Hanson, “Coupled vibration-dissociation time-histories and rate measurements in shock-heated, nondilute O₂ and O₂–Ar mixtures from 6000 to 14000 K,” *Phys. Fluids* **33**, 056107 (2021).
<https://doi.org/10.1063/5.0048059>
13. A. Farooq, J. B. Jeffries, and R. K. Hanson, “Sensitive detection of temperature behind reflected shock waves using wavelength modulation spectroscopy of CO₂ near 2.7 μm,” *Appl. Phys. B* **96**, 161–173 (2009).
14. E. Kustova and M. Mekhonoshina, “Multi-temperature vibrational energy relaxation rates in CO₂,” *Phys. Fluids* **32**, 096101 (2020).
<https://doi.org/10.1063/5.0021654>
15. N. B. Vargaftik, *Tables on the Thermophysical Properties of Liquids and Gases* (Nauka, Moscow, 1972; Hemisphere, Washington, DC, 1975).
16. R. D. Trengove and W. A. Wakeham, “The viscosity of carbon dioxide, methane, and sulfur hexafluoride in the limit of zero density,” *J. Phys. Chem. Ref. Data* **16**, 175 (1987).
<https://doi.org/10.1063/1.555777>
17. *Handbook of Physical Quantities*, Ed. by I. S. Grigoriev and E. Z. Meilikhov (Energoatomizdat, Moscow, 1991; CRC, Boca Raton, Fla., 1995).

Translated by O. Pismenov